Talanta 215 (2020) 120939

Contents lists available at ScienceDirect

Talanta

journal homepage: www.elsevier.com/locate/talanta

Nanozyme-based sensing platforms for detection of toxic mercury ions: An alternative approach to conventional methods

Anwarul Hasan[a,b,**], Nadir Mustafa Qadir Nanakali[c,d], Abbas Salihi[e], Behnam Rasti[f], Majid Sharifi[g,h], Farnoosh Attar[i], Hossein Derakhshankhah[j], Inaam Ahmad Mustafa[e], Shang Ziyad Abdulqadir[e], Mojtaba Falahati[g,*]

[a] Department of Mechanical and Industrial Engineering, College of Engineering, Qatar University, Doha, 2713, Qatar
[b] Biomedical Research Center, Qatar University, Doha, 2713, Qatar
[c] Department of Biology, College of Education, Salahaddin University-Erbil, Kurdistan Region, Iraq
[d] Department of Biology, College of Science, Cihan University-Erbil, Iraq
[e] Department of Biology, College of Science, Salahaddin University-Erbil, Kurdistan Region, Iraq
[f] Department of Microbiology, Faculty of Basic Sciences, Lahijan Branch, Islamic Azad University (IAU), Lahijan, Guilan, Iran
[g] Department of Nanotechnology, Faculty of Advanced Sciences and Technology, Tehran Medical Sciences, Islamic Azad University, Tehran, Iran
[h] Department of Animal Science, Faculty of Agriculture, University of Tabriz, Tabriz, Iran
[i] Department of Biology, Faculty of Food Industry and Agriculture, Standard Research Institute (SRI), Karaj, Iran
[j] Pharmaceutical Sciences Research Center, Kermanshah University of Medical Sciences, Kermanshah, Iran

ARTICLE INFO

Keywords:
Mercury
Toxicity
Detection
Nanozymes
Gold
Platinum

ABSTRACT

Mercury (Hg) is known as a poisonous heavy metal which stimulates a wide range of adverse effects on the human health. Therefore, development of some feasible, practical and highly sensitive platforms would be desirable in determination of Hg^{2+} level as low as nmol L^{-1} or pmol L^{-1}. Different approaches such as ICP-MS, AAS/AES, and nanomaterial-based nanobiosensors have been manipulated for determination of Hg^{2+} level. However, these approaches suffer from expensive instruments and complicated sample preparation. Recently, nanozymes have been assembled to address some disadvantages of conventional methods in the detection of Hg^{2+}. Along with the outstanding progress in nanotechnology and computational approaches, pronounced improvement has been attained in the field of nanozymes, recently. To accentuate these progresses, this review presents an overview on the different reports of Hg^{2+}-induced toxicity on the different tissues followed by various conventional approaches validated for the determination of Hg^{2+} level. Afterwards, different types of nanozymes like AuNPs, PtNPs for quantitative detection of Hg^{2+} were surveyed. Finally, the current challenges and the future directions were explored to alleviate the limitation of nanozyme-based platforms with potential engineering in detection of heavy metals, namely Hg^{2+}. The current overview can provide outstanding information to develop nano-based platforms for improvement of LOD and LOQ of analytical methods in sensitive detection of Hg^{2+} and other heavy metals.

1. Introduction

Mercury (Hg) is known as one of the most frequent noxious metals in nature and extensively exists in water, soil, and unexpectedly food. The high levels of Hg^{2+} are globally produced from natural events and man-made occupations such as power plants, burning of coal, oil and wood, industrial processes, and metal mining [1]. Interaction of Hg^{2+} with biological systems results in serious adverse effects against the tissues and immune cells, even at low levels, and its accumulation in the tissues can lead to several disorders such as neuropathic disorders [2], cardiovascular disorders [3], recognition memory impairments [4], variations in the salivary glands [5], hippocampal dysfunction [6], psychiatric-like disorders [7], membranous nephropathy [8], and even death [9]. Since the acute toxicity of Hg^{2+} is well-documented, the

Abbreviations: AAS/AES, Atomic absorption/emission spectrometry; GCE, Glassy carbon electrode; AuNPs, Gold nanoparticles; GO, Graphene oxide; ICP-MS, Inductively coupled plasma-mass spectrometry; LOD, Limit of detection; LOQ, Limit of quantification; Hg, Mercury; NPs, Nanoparticles; Pt, Platinum

* Corresponding author.
** Corresponding author. Department of Mechanical and Industrial Engineering, College of Engineering, Qatar University, Doha 2713, Qatar.
E-mail addresses: hasan.anwarul.mit@gmail.com, ahasan@qu.edu.qa (A. Hasan), mojtaba.falahati@alumni.ut.ac.ir (M. Falahati).

https://doi.org/10.1016/j.talanta.2020.120939
Received 4 December 2019; Received in revised form 13 March 2020; Accepted 14 March 2020
Available online 17 March 2020

World Health Organization (WHO) and the U.S. Environmental Protection Agency (EPA) have, respectively, announced that the maximum approved levels of Hg^{2+} in water should be 6 and 2 μg L^{-1} [10]. Therefore, it seems necessary to apply some approaches to sense Hg^{2+} at very low levels down to nmol L^{-1}.

The most common Hg^{2+} detection methods are AAS/AES, cold vapor AAS, electrochemical methods, gas and liquid chromatography, and high performance chromatography [11]. Since these methods demonstrate low sensitivity, expensive equipment, and time-consuming as well as complex preparation processes, the application of NP-based methods has received a great deal of attention, recently [12]. Currently, some procedures are applied for Hg^{2+} sensing such as ICP-MS and AAS/AES. Also, a number of nanomaterials have been used to assemble different sensors toward Hg^{2+} detection in the field [13–15]. Moreover, several new methods have been assembled for Hg^{2+} detection using several NPs such as Au [16,17], Pt [18,19], and GO [20,21] based on their intrinsic catalytic performance. These nanomaterials with intrinsic catalytic activity, called nanozymes, show similar performance to that of native enzymes. Consequently, nanozymes can be applied to detect Hg^{2+} level based on the variations in the colorimetric or fluorogenic reactions. In this paper we will review all applicable methods for Hg^{2+} detection and will discuss the principle of each assembly. We will show that despite all classical-based assemblies providing potential analytical activity for Hg^{2+} detection; they are subjected to high-cost and complex surface functionalization, which needs complicated analytical tools. Accordingly, the assembly of feasible, low-cost, and highly sensitive and selective sensors based on nanozymes may develop promising alternative platforms in determination of Hg^{2+} level. Therefore, we will overview the toxicity of Hg^{2+} on the biological systems followed by provided details of the various platforms such as ICP-MS, AAS/AES, nanomaterial-based nanobiosensors, and nanozymes used for Hg^{2+} detection.

2. Mercury toxicity

Hg^{2+} is constantly exposed to human through contaminated rain, marine water, coal, vegetables, and food chain and stimulates some adverse effects on the human health [22–25]. Immense examination have been carried out on people across the world who frequently intake fish products. These people are at an enhanced risk of Hg^{2+} poisoning. Fetus and children are more sensitive to side effects of Hg^{2+} [26,27]. Change in neuro motor functions [28] and memory loss [28,29] have been determined among children exposed to low levels of Hg^{2+}. Also, neuronal damage [30], multiple sclerosis [31], Alzheimer's disease [32], and hippocampal dysfunction and cognitive impairment [6] were reported in adults upon exposure to low levels of Hg^{2+}. It has been reported that mitochondria of the neurons is considered as the site of the injury induced by Hg^{2+} [33]. Also, it has been reported that Hg^{2+} interrupts the regeneration of neurons via inhibition of microtubule polymerization [34].

In another study, oxidative stress, apoptosis induction and cleavage of rho-associated, coiled-coil-containing protein kinase 1 (ROCK-1) have been reported to play an important role in Hg^{2+}-induced cell mortality in astroglial cells (Fig. 1A) [35]. Similarly, oxidative stress, neural cell mortality, and functional deficits have been reported after exposure to Hg^{2+} [36]. It has been also displayed that low levels of Hg^{2+} in rats induced oxidative stress, loss of neuroprotection, and motor function [37]. Regarding heart function, it has been revealed that chronic Hg^{2+} exposure disables sympathovagal balance of the rat heart [38] and induces heart rate irregularity [39]. Exposure of virgin rats to acute exposure of Hg^{2+} resulted in remarkable inflammatory infiltration and serious morphological changes, such as glomeruli atrophy, dilatation of Bowman's capsule, tubular damage, and hepatocytes mortality. Furthermore, these rats showed some remarkable changes such as mitochondrial alteration, oxidative stress, and activation of stress proteins at both kidney and liver tissues [40]. It was also shown that chronic exposure of Hg^{2+} can damage kidney, liver, and brain in rats, while vitamin C can mitigate the Hg^{2+}-induced toxicity [41]. It was also declared that high level of blood Hg^{2+} is associated with reduction in liver function in elderly populations [42]. However, these Hg^{2+}-induced liver damages are gender sensitive (Fig. 1B)[43]. It was also demonstrated that Hg^{2+} contamination by lightning creams may increase some adverse effects against normal tissues [44]. Indeed, the source of Hg^{2+}, routs of the exposure, Hg^{2+} level and the type of tissue can determine the severity of Hg^{2+}-induced toxicity.

Moreover, it has been indicated that reproductive impairment can be seen in rats exposed to a low level of Hg2+ [45]. Besides, it was reported that high levels of Hg^{2+} result in infertility or subfertility, induction of menstrual and hormonal diseases, and reduction of semen quality index [46]. Furthermore, hypertension [47] and cancer promotion [48] have been also reported in the literature about Hg^{2+} toxicity. Based on the significant Hg^{2+}-induced toxicities, development of some potential systems for the Hg^{2+} detection at very low levels would be promising. In the following sections we will review the advantages and disadvantages of several approaches commonly used for Hg^{2+} detection.

3. Inductively coupled plasma mass spectrometry (ICP-MS)

ICP-MS can be applied to sense metals and a number of non-metals at levels down to 10^{-15} M. Fang et al. [49] reported using reversed phase chromatography based on ICP-MS approach for simultaneous detections of arsenic and Hg^{2+}in rice flour. The LODs of the examined species were reported to be in the range of 0.84–2.41 μg L^{-1} for arsenic and 0.01–0.04 μg L^{-1} for Hg^{2+}, respectively [49]. Ma et al. [50] synthesized functionalized magnetic NPs for adsorption of Hg^{2+}species in water and human hair trials. Then, a procedure of magnetic solid phase extraction integrated with ICP-MS was assembled for the detection of methyl Hg and Hg^{2+}. The authors reported LOD for methyl Hg and Hg^{2+} to be 1.6 and 1.9 ng L^{-1}, respectively (Fig. 2A) [50]. Other reports for the determination of Hg^{2+} level using the ICP-MS technique are listed in Table 1.

4. Atomic absorption/emission spectrometry

AES/AAS is known as a spectro-analytical tool for the quantitative assay of chemical elements applying the absorption/emission of light by the gaseous status of atom. Panichev and Panicheva [51] developed a procedure for the sensing of Hg^{2+}in seafoods that depends on the direct thermal evaporation of Hg^{2+}. The LOD and the limit of quantification for the sensing of Hg^{2+} in wet fish trials were 0.6 ng g^{-1} and 2.0 ng g^{-1}, respectively. Almeida et al. [52] reported a simple and effective route for Hg^{2+} extraction with Universol® in soil and sediment specimen integrated with the cold vapor generation AAS technique. The LOD were found to be 0.07 and 0.08 mg kg^{-1} for Hg_{total} and Hg^{2+}, respectively. Zhang et al. [53] demonstrated a feasible, non-chromatographic and bio-analytical procedure for the sensing of Hg^{2+} in water and biological samples. Hg^{o} was formed by utilizing formic acid and ultraviolet or ultrasonic radiation, and was then analyzed by AES. The LOD was 0.005 and 0.01 μg L^{-1} for total Hg and Hg^{2+}, respectively (Fig. 2B) [53]. Some other data that have been used for the sensing of Hg^{2+} using AAS/AES technique are tabulated in Table 2.

As summarized in Sections 1.1 and 1.2, ICP-MS and ASS/AES methods demonstrate excellent sensitivity and selectivity, however, they are highly-priced and need complicated equipment, instructed operators, and prolonged sample preparation, which restrict their potential implementation for on-site investigations. Therefore, the assembly and development of simple and cost-effective sensors for on-site detection of Hg^{2+} is highly demanded. The application of NPs can be useful as an alternative route for simple, low-cost, and highly sensitive detection of Hg^{2+}.

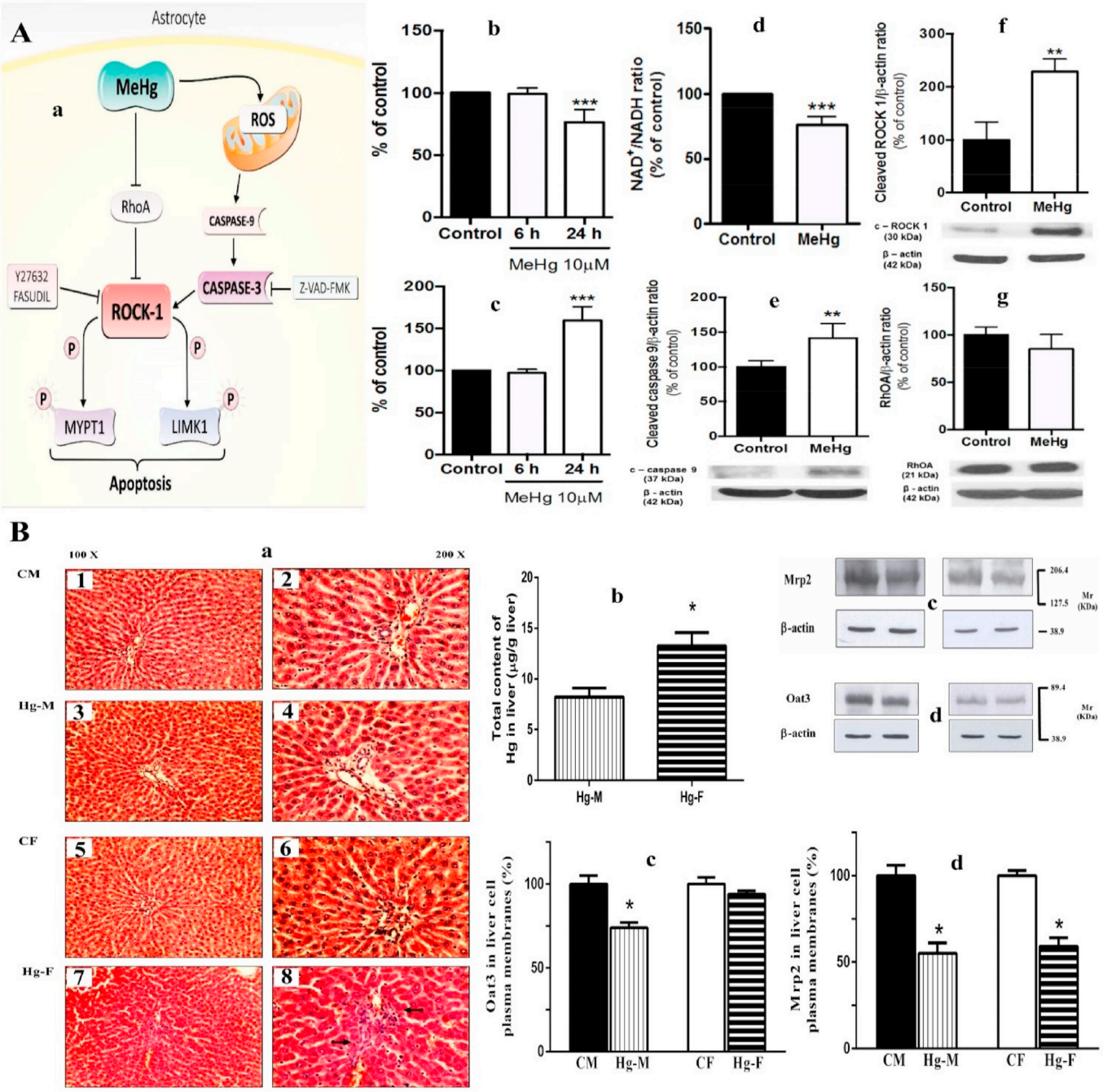

Fig. 1. A: Oxidative stress, caspase-3 activation and cleavage of ROCK-1 play an essential role in MeHg-induced cell death in primary astroglial cells. a; A proposed model for MeHg-mediated mitochondrial injury, ROCK-1 activation and apoptosis in primary culture of mouse astrocytes. b-c; Time-dependent MeHg-induced cytotoxicity in primary culture of mouse astrocytes. Astrocytes were exposed to vehicle (black bars) and 10 μM MeHg for 6 h and 24 h. (b) Cell viability was evaluated by ATP assay and (c) LDH release. d; MeHg exposure induces a decrease in the NAD^+ production in primary culture of mouse astrocytes. The ratio of NAD^+/NADH was calculated as (NADt-NADH)/NADH. e; MeHg exposure induces caspase-9 activation in primary culture of mouse astrocytes. Astrocytes were exposed to vehicle or to 10 μM MeHg for 6 h f; MeHg exposure induces ROCK-1 cleavage/activation in primary cultures of mouse astrocytes. g; MeHg exposure induces decrease in RhoA expression (1 h) before the onset of caspase-3 activation (6 h) in primary culture of mouse astrocytes [35]. **B: Gender differences in Hg-induced hepatotoxicity: Potential Mechanisms.** a; Representative micrographs of liver sections with hematoxylin/eosin-stained from male (1, 2, 3 and 4) and female (5, 6, 7 and 8) rats. After 18 h of a level of $HgCl_2$ (4 mg kg^{-1} body weight, i.p), females showed a notable disorganization on the radial pattern of hepatocytes and dispersed areas of fibrosis (arrow). In Hg^{2+}-treated males, the microscopic changes were less than Hg^{2+}-treated females. CM: Control males, Hg-M: Hg^{2+}-treated males, CF: Control females, Hg–F: Hg^{2+}-treated females. b; Content of total Hg^{2+} in liver from Hg-M and Hg–F. c; Immunoblotting analyses for Oat3 in liver total plasma membranes from CM, Hg-M, CF and Hg–F. Kaleidoscope Pre-stained Standards of molecular mass corresponding to bovine serum albumin (89.4 kDa) and to carbonic anhydrase (38.9 kDa) are indicated in the right of the immunoblotting bands. d; Immunoblotting analyses for Mrp2 in liver total plasma membranes from CM, Hg-M, CF and Hg–F. Kaleidoscope Pre-stained Standards of molecular mass corresponding to myosin (206.4 kDa), β-Galactosidase (127.5 kDa) and to carbonic anhydrase (38.9 kDa) are indicated in the right of the immunoblotting bands [43].

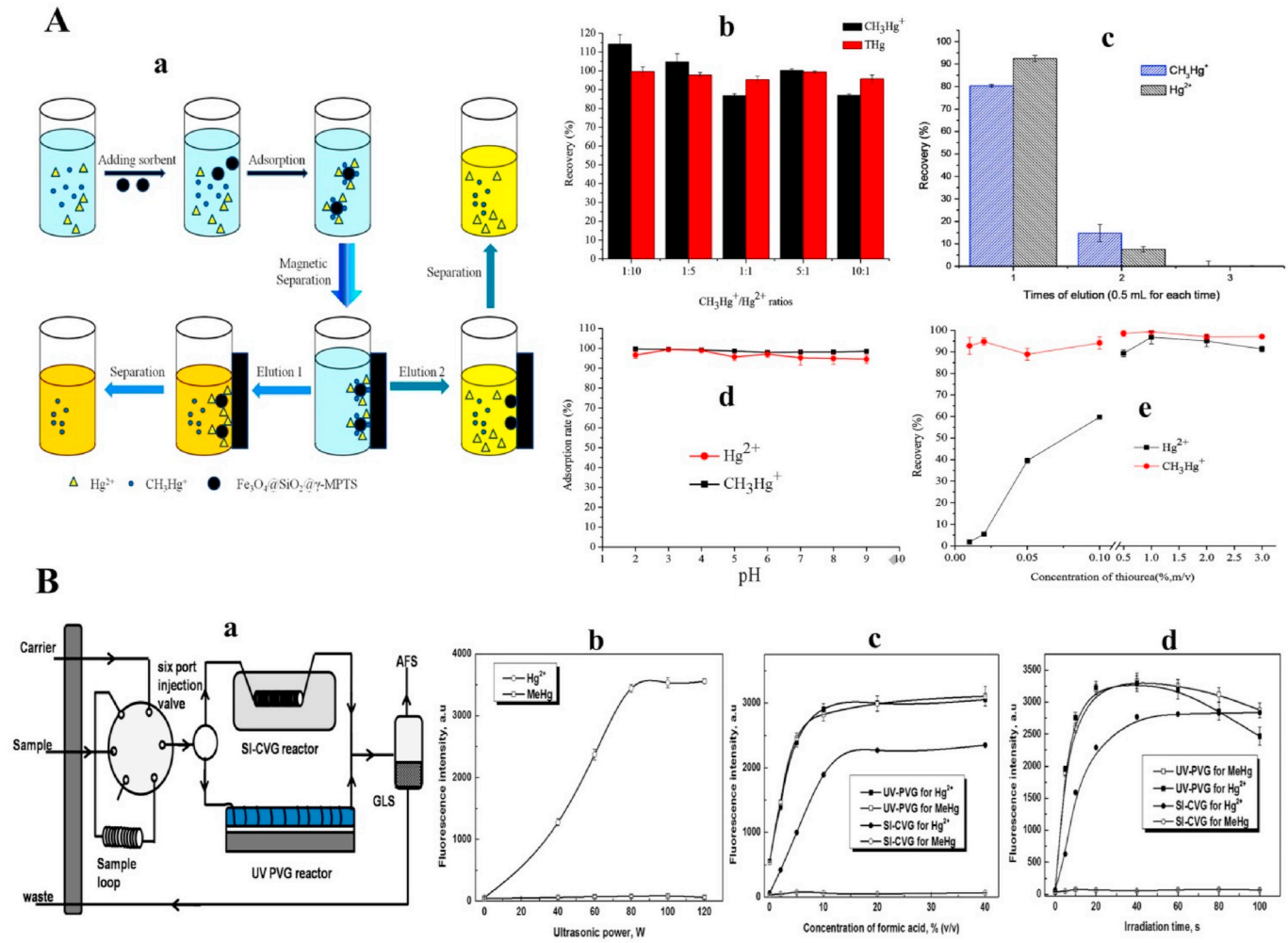

Fig. 2. A: Magnetic solid phase extraction coupled with plasma mass spectrometry for the speciation of Hg^{2+} in samples. a; CH_3Hg^+ and Hg^{2+} exhibited similar adsorption and different desorption behavior on Fe_3O_4@SiO_2@γ-MPTS. b; Effect of the CH_3Hg^+/Hg^{2+} ratio on the recovery of CH_3Hg^+ and THg. c; Effect of the elution volume on the recovery of CH_3Hg^+ and Hg^{2+} (20 μg L^{-1}). d; Effect of pH on the sorption percentage of Hg^{2+} and CH_3Hg^+ (20 μg L^{-1}) on the Fe_3O_4@SiO_2@γ-MPTS. e; Effect of thiourea concentration in 1.5 M HCl on the recovery of Hg^{2+} and CH_3Hg^+ (20 μg L^{-1}) [50]. **B: Application of flow injection–green chemical vapor generation–atomic fluorescence spectrometry to detection of Hg^{2+} in samples.** a; Schematic of the experimental setup. b; Effect of ultrasonic power on AFS response. c; Effect of formic acid on AFS response. d; Effect of irradiation time on AFS response [53].

5. Nanomaterials

To overcome the above-mentioned limitations, a number of nanomaterials have been employed to assemble nano-based sensors for Hg^{2+} detection in different fields. Frequent detection approaches for selective and subtle sensing require surface functionalization of nanomaterials with different moieties. In the following sections we will review some of the recent papers on the modification of nanomaterials and their subsequent applications in Hg^{2+} detection.

5.1. NPs/oligonucleotides

In recent years, the interaction between Hg^{2+} and bisthymine (T-T) has received a great deal of interest in detection of heavy metals [54,55]. Indeed, T–T mismatch, as an Hg-specific oligonucleotide (MSO) can bind with Hg^{2+} in a selective and strong manner [56,57].

Table 1
Detection of Hg^{2+} using ICP-MS technique.

Analytical tools	Sample	LOD for Hg^{2+}	Ref.
Liquid chromatography ICP-MS	Fish oils	0.5–1 ng g^{-1}	[109]
Sector field ICP-MS	Hair of school children from a polluted area	0.20–0.25 mg kg^{-1}	[110]
High pressure liquid chromatography ICP-MS	Water and fish samples	0.49–0.74 ng L^{-1}	[111]
Isotope dilution – ICP-MS	Microalgae	9 pg	[112]
ICP-MS	Peach and jujube	0.0003 (peach) to 0.0016 (jujube)pg	[113]
Ion-pairing reversed-phase chromatography coupled to ICP-MS	Freshwater fish	0.015 μg L^{-1}	[114]
Nanoliter liquid chromatography and ICP-MS with an in-column high-pressure nebulizer	Caprine blood	0.044–0.13 μg L^{-1}	[115]
Electrothermal vaporizer with ICP-MS	Soil	3.1 ng g^{-1}	[116]

Table 2
Detection of Hg^{2+} using AAS/AES technique.

Analytical tools	Sample	LOD for Hg^{2+}	Ref.
Photochemical vapor generation graphite furnace AAS	Fish tissue	0.31–3.17 μg L^{-1}	[117]
Flow injection catalytic cold vapor AAS	Urine samples	0.14 μg L^{-1}	[118]
Cold vapor AAS	Water and fish samples	10 ng L^{-1}	[119]
Amberlite XAD-4 column integrated with flow injection cold vapor generation AAS	Water and fish tissue	0.148 μg L^{-1}	[120]
Thermal decomposition AAS	Fish tissue	0.2 μg kg^{-1}	[121]
AES	Lake water samples	3 ng L^{-1}	[122]
Ultraviolet atomization-AES	Spiked environmental water	0.015 mg L^{-1}	[123]
Cold vapor microwave plasma-AES	Wild Atlantic salmon muscle tissue	0.22 μg L^{-1}	[124]

Therefore, T-rich sequence can be designed to selectively bind with Hg^{2+}. Based on this interaction, Cui et al. [58] developed a fluorescent nanobiosensor based on carbon dots (CDs)-tagged oligo-deoxy ribonucleotide (ODN) and GO (Fig. 3A) as a quencher of Hg^{2+}. The LOD was in the range of 5–200 nmol L^{-1}. Wordofa et al. [59] assembled a label-free chemiresistorive nanobiosensor for the sensing of Hg^{2+} utilizing DNA-modified single walled carbon nanotubes (SWNTs). Upon the formation of T–Hg^{2+}–T and subsequent release of poly-A, an alteration in the resistance of the chemiresistive nanobiosensor is detected, which is employed to calculate the level of Hg^{2+} [59]. The LOD for CH_3Hg^+ ions based on this nanobiosensor was in the range of 0.5–100 nmol L^{-1}.

Memon et al. developed a colorimetric detection of Hg^{2+} by using SSDNA oligonucleotides and AuNPs [62]. As a result, T–Hg^{2+}–T domain as a dsDNA, cannot attach on the AuNPs. This leads to agglomeration of the NPs which can be detected by dynamic light scattering as alteration in the particle hydrodynamic radius [60]. Therefore, the authors suggested a rational assembly for the MSO with a significant enhancement in sensing sensitivity. The LOD dropped to 15 nmol L^{-1} and the linear range was from 50 to 300 nmol L^{-1} for Hg^{2+} [60]. Other investigations utilized for the detection of Hg^{2+}using NPs/oligonucleotides approach are summarized in Table 3. Finally, despite the appropriate detection and potential sensitivity of oligonucleotide in Hg^{2+} detection, further investigations are needed to overcome the complexity of oligonucleotide-based nanobiosensor fabrication and limited diagnosis resulted from mismatch between the probe and the target.

5.2. NPs/thiol compounds

Thiol groups provide a strong binding affinity to Au and Hg^{2+}. Asadpour-Zeynali and Amini [61] developed a voltammetric nanobiosensor for determination of Hg^{2+} level using a mercapto-carboxylic acid intercalated coated paired hydroxide NP-improved electrode with a LOD of 0.8 nmol L^{-1}. Devi et al. [62], using AuNPs-loaded rGO-SH GCE, were able to design a GCE/rGO-SH/Au-NPs electrode to detect Hg^{2+} with a LOD of 0.2 μM based on the electrochemical method. Sharma et al. [63] developed a feasible and selective strategy for the optical sensing of Hg^{2+} in water employing thiol terminated chitosan (Ch) functionalized AgNPs at different pH (Fig. 3B). The color of the Ch-AgNPs changes after interaction with Hg^{2+} and the LOD was calculated to be 5 μg L^{-1} [63]. Other reports for the detection of Hg^{2+} using the NPs/thiol compounds approach are listed in Table 4.

Surface modification of nanomaterials have also been done by different moieties such as proteins/peptides [64], polymers [14,65–67], aptamers [68–70] and cysteine [71], which lead to selective binding of Hg^{2+} and fortifying the signal transduction based on the level of Hg^{2+}. All of these approaches require a complicated sample preparation and advanced analytical devices for readouts. Indeed, NPs should be functionalized with different moieties in order to increase the selectivity and sensitivity of the assemblies which needs time consuming and expensive procedures. The ion interference may also occur and should be overcome by coupling formation between functional groups. To address these disadvantages, the nanozyme-based platforms were introduced as uncomplicated, affordable, and highly sensitive and selective nano-based sensors for on-site detection of Hg^{2+}.

5.3. Covalent organic frameworks in Hg^{2+} detection

Some of the major challenges in the determination of Hg^{2+} levels by nanomaterial are the lack of accuracy, precision, and sensitivity compared to conventional methods. In this regard, covalent organic framework (COFs) with different recognition methods such as chromatography, membrane separation and solid-phase extraction can be used to improve the selective framework based sensor toward Hg^{2+} detection [72]. This technique uses two- or three-dimensional porous crystals formed through strong covalent bonds. COFs structure due to symmetry and rigid geometry with desirable topology such as individual configurable sponginess, well-organized channels, optional building blocks, expectable state of structures, easy process, large reaction areas, and thermal as well as chemical stability provide potential properties for sensing systems [73]. In this regard, due to the decreased catalytic activity of AuNPs resulted from their agglomeration, Li et al. [74] by using COF structure from 1,3,5-Tris-(4-formyl-phenyl)triazine and 4, 4′-azodianiline polymers not only increased the stability and peroxidase-like activity of AuNPs, but also enhanced the LOD of Hg^{2+} up to 0.75 nmol L^{-1} with a linear amplitude of 5–300 nmol L^{-1}. The constructed COF-AuNPs sensor provided high sensitivity and selectivity in detection of Hg^{2+}. Likewise, He et al. [75] by producing COF colorimetric sensors based on triarylamine polymer and Suzuki polymerization, in addition to Hg^{2+} detection with a LOD of 22.8 μg L^{-1}, were able to remove Hg^{2+} up to 95%. Recently, Guo et al. [76] designed two-dimensional COF containing N-doped CDs (NCDs) and Rhodamine B (RhB) nanocomposites (NCDs-RhB@COF) that were able to detect Hg^{2+} based on a colorimetric sensors with a LOD of 3 15.9 nmol L^{-1} and a linear range of 0.048–10 μM. These fluorescent-based nanobiosensors can be considered as a promising platform in industrial activities because of their promising sensitivity and stability. Taken together, COFs-based nanobiosensors can be utilized to develop a simple Hg^{2+} with high sensitivity, accuracy, stability and reproducibility in real samples.

6. Nanozymes

Enzymes as biological catalysts can speed up the conversion of substrates into products in biochemical pathways. Enzymes are composed of amino acids, which allow them to reach their high catalytic activity and maximum catalytic performance under physiological conditions. Nevertheless, enzymes lose their activity after subjection to harsh conditions such as acidic or basic pH, high temperature, and the presence of denaturant and/or proteases which considerably hamper their actual implementation in industry [77]. To overcome these restrictions, there is a growing demand to use enzyme mimetics which are more vigorous than proteins and affordable at lower-cost to fabricate [78]. The major part of enzyme mimetics is the utilization of organic chemical compounds as the functional core. Furthermore, non-protein biomolecules with enzyme-like performance have been identified, such as Ribozymes [79], Abzymes [80] and DNAzymes [81]. However, most

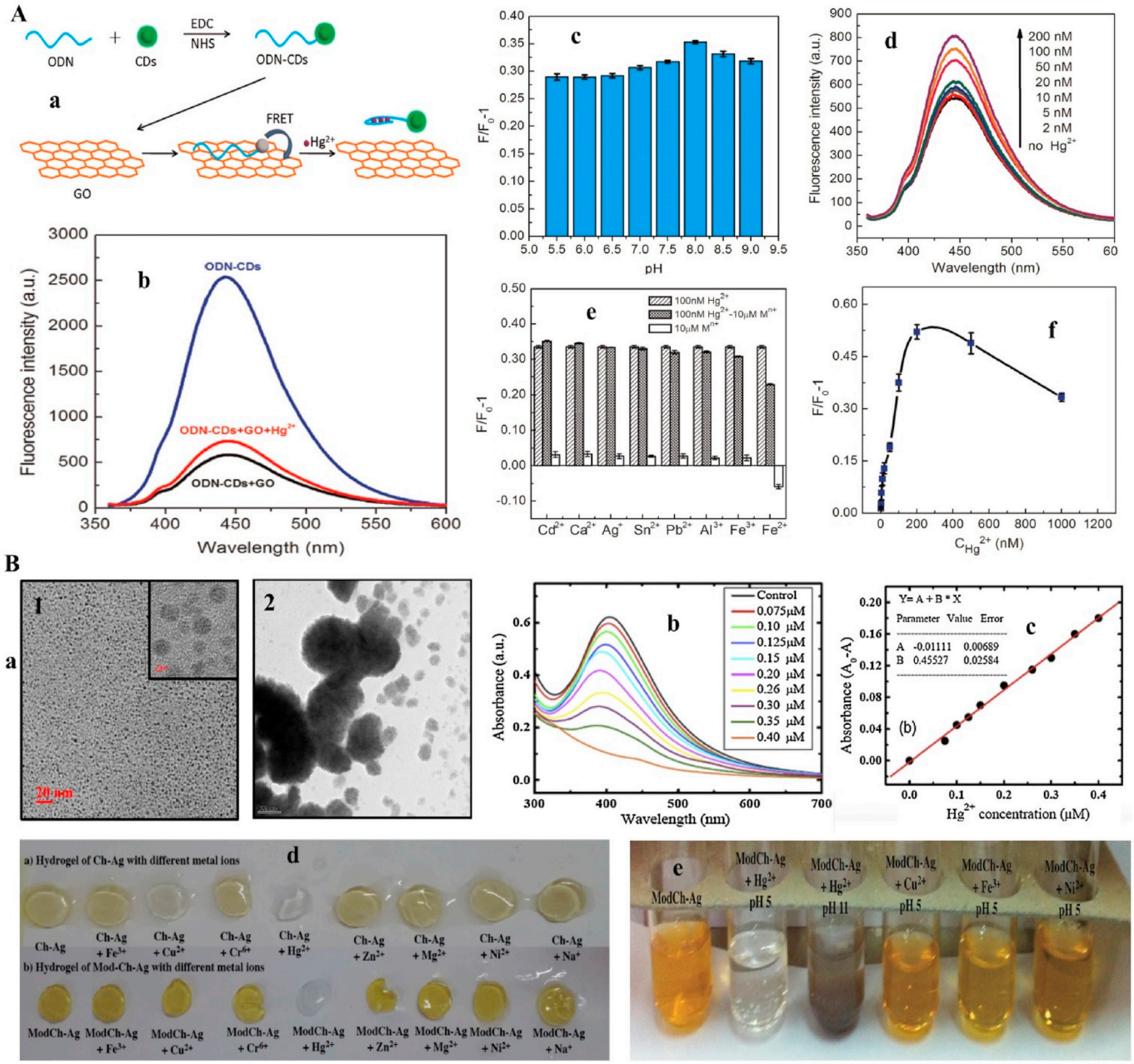

Fig. 3. A: a fluorescent biosensor based on CDs-labeled oligodeoxy ribonucleotide and GO for Hg detection. a; Schematic illustration of the GO-based sensor system for Hg^{2+} detection. b; The fluorescence spectra of ODN–CDs and GO-based sensor system in the presence or absence of Hg^{2+}. c; Effect of pH on the F/F_0-1 value of sensor system. d; Fluorescence spectra of the GO-based sensor system containing various levels (0, 2, 5, 10, 20, 50, 100, and 200) of Hg^{2+}. e; electivity of the sensing system of Hg^{2+} to other competing metal ions, 100 nM Hg^{2+} and 10 μM other metal ions. f; Plot of the F/F_0-1 value as a function of the Hg^{2+} level [58]. **B: Thiol terminated chitosan capped AgNPs for sensitive and selective detection of Hg^{2+} (II) ions in water.** a; TEM images of the Mod-Ch-AgNPS in the (1) absence (high-resolution in the inset) and (2) presence of Hg^{2+}. b; Change in the UV–vis spectra of Mod-Ch-AgNPs upon the addition of increasing level of Hg^{2+} (0–0.4 μM). c; Plot of absorbance intensity versus Hg^{2+} level. d; Photographs of hydrogel of (a) Ch-AgNPs and (b) Mod-Ch-AgNPs in presence of different metal ions. e; Photograph showing the effect of pH for the separation of Hg^{2+} from water using Mod-Ch-AgNPs [63].

Table 3
Detection of $Hg2^{+}$ using NPs/oligonucleotides approach.

Analytical tools	Detection strategy	LOD for Hg^{2+}	Ref.
Self-assembling Hg- oligonucleotide-AuNPs modified indium tin oxide (ITO) electrode	Electro- chemiluminescence	5.1 pmol L^{-1}	[125]
Guanine nanowire	Electrochemical sensor	33 pmol L^{-1}	[126]
SsDNA/nano-graphite	Fluorescence	3 nmol L^{-1}	[127]
DNA self-assembled Au nano-rods	colorimetric	3.2 nmol L^{-1}	[128]
Au NRs@T	SERS	0.1 nmol L^{-1}	[129]
GO-Au modified electrode integrated with AuNPs	Electrochemical	0.001 amol L^{-1}	[130]

Table 4
Detection of $Hg2^{+}$ using NPs/thiol compounds approach.

Analytical tools	Detection strategy	LOD for $Hg2^{+}$	Ref.
Thiol-functionalized silver (Ag) NPs	SERS	0.0024 μmol L^{-1}	[131]
AuNPs- thiocyanuric acid	colorimetric aptasensor	0.5 nmol L^{-1}	[132]
Thiol-functionalized polysiloxanes modified by lead NPs	Voltammetric sensor	0.35 nmol L^{-1}	[133]
Nitrogen-doped, thiol-functionalized CDs	Fluorescence	6.8 nmol L^{-1}	[134]
Au, Hexanedithiol and Rhodamine B nanocomposite	Absorption and fluorescence	0.5 ng mL-1	[135]
Tween 20-modified Au nanorods-DTT	Spectrometric, aggregation	0.42 pmol L^{-1}	[136]

enzyme mimetics are still restricted in industrial implementation because of their low efficiency and selectivity. Therefore, nanozymes, as a brand-new kind of enzyme mimetic, are considered as nanomaterials with innate enzyme-like performance that can effectively catalyze the reactions and show identical kinetics and mechanisms of native enzymes under physiological conditions.

The enzyme-like activities of nanozymes derive from the nanomaterial itself, rather than combining auxiliary enzymes onto the nanomaterial. Nanozymes present a great deal of benefits in industry because their bioactivity cannot be easily reduced and digested by proteases [82]. In addition, the catalytic activity of nanozymes can be controlled by adjusting their physicochemical features, similar to the properties of NPs that usually depend on dimension, morphology, chemical composition, and functional groups. This represents an advantage for using nanozymes over other classical enzyme mimetics. Currently, there are a number of nanomaterials that have been determined to provide intrinsic activity close to enzymes such as peroxidases [83], catalase [84], esterase [85] and others. Also, some nanozymes like iron NPs provide two intrinsic features, namely magnetic properties and peroxidase-like performance. This functional duality can be utilized in both separation of iron molecules from water and potential catalyst for enzymatic reactions. Therefore, the adaptability and stability of nanozymes cause extensive new practical applications in chemistry, biotechnology and medicine.

Nanomaterials are chemically inert in biological media and can be considered as bioactive molecules. Nanomaterials are synthesized via different methods, such as physical, chemical and biological fabrications [86], to produce nanozymes with different characteristics for catalytic applications [87], antibacterial applications [88], ultrasensitive cancer diagnosis [89], detection [90], and determination of heavy metals level in environment [91]. It is indicated that nanozymes may display the next generation of artificial enzymes. Therefore, the nanozyme model – introducing nanomaterials with inherent enzymatic performance – can lead to a newly prominent branch that bridges nanotechnology and biology to medicine. In this chapter we try to overview some recent applications of nanozymes such as AuNPs, PtNPs and others in detecting heavy metals such as Hg^{2+}.

6.1. AuNPs

Han et al. [92], assembled a simple Au nanozyme-derived paper chip (AuNZ-PAD) that showed a high level of sensitivity and selectivity to on-site detection of Hg^{2+}. The colorimetric detection of Hg^{2+} by using AuNZ-PAD chip was developed based on the enzyme-like performance of AuNPs fortified by the presence of Au–Hg^{2+}. In this case, highly sensitive determination of Hg^{2+} level was observed, demonstrating the practicability of this system for the sensing of Hg^{2+} in real samples integrated with a smartphone camera [92]. Zhao et al. [93], manipulated a system for the colorimetric assay of Hg^{2+} based on the observable signal intensification stimulated by a Cu@Au–Hg^{2+} trimetallic nanohybrid with peroxidase-like activity with a LOD of 3.0 nmol L^{-1}.

Zohora et al. [94] biosynthesized AuNPs and showed that ester-like phytochemicals exist on the surface of AuNPs, leading to determination of Hg^{2+} level with a LOD of 1.44 μM. Huang et al. [16] used protamine-AuNPs with peroxidase-like activity for the specific and sensitive colorimetric assessment of Hg^{2+} with a LOD of 1.16 nmol L^{-1}. Jiang et al. [95] reported a colorimetric sensing of Hg^{2+} based on the enzyme-like function of chitosan-AuNPs with a LOD of 20 nmol L^{-1}. Wang et al. [96] also reported colorimetric analysis of Hg^{2+} by the Hg^{2+}-stimulated peroxidase mimicking performance of a nanohybrid fabricated from graphitic carbon nitride and AuNPs with a LOD of 3.0 nmol L^{-1}. Ma et al. [91] developed a nanosystem to perform the colorimetric assay for sensitive assay of Hg^{2+} by molybdenum disulfide (MoS_2)–Au nanocomposites as peroxidase mimetics (Fig. 4A). The presence of Hg^{2+} increases the peroxidase-like function of nanohybrid, resulting in the direct assay of Hg^{2+} with a LOD down to 5 nmol L^{-1}.

6.2. PtNPs

Li et al. [97] used BSA to act as the nucleation template for fabrication of Pt nanozymes (2 nm), showing the outstanding peroxidase-like performance. Interestingly, Hg^{2+} was able to inhibit the enzymatic function of Pt nanozymes, mainly through the reactions with PtNPs. Therefore, it was possible to develop a colorimetric Hg^{2+} sensing platform employing the peroxidase mimicking performances of PtNPs [98]. It was shown that BSA-stabilized Pt nanozymes displayed a great deal of possibility to detect Hg^{2+} without remarkable intervention (Fig. 4B) with a LOD of 7.2 nmol L^{-1} and the linear response range of 0–120 nmol L^{-1} [97].

Zhou and Ma [99] reported that PtNPs can be used as a nanozyme for fluorescent and colorimetric dual sensing of Hg^{2+} by oxidation of o-phenylenediamine with LODs of 0.14 nmol L^{-1} and 0.8 nmol L^{-1}, respectively. Li et al. [100] also reported that PtNPs encapsulated metal–organic frameworks can be employed for colorimetric sensing of Hg^{2+} with a LOD of 0.35 nmol L^{-1}. Peng et al. [19] used core-shell Au@Pt NPs for simultaneous colorimetric determination of Hg^{2+} and Ag^{+} levels with LODs of 3.5 nmol $L^{-1}$and 2.0 nmol L^{-1}, respectively. Wang et al. [101] developed a nanohybrid that is composed of graphitic carbon nitride functionalized PtNPs for simple and specific colorimetric determination of Hg^{2+} level with a LOD of 1.23 nmol L^{-1}. Guo et al. [102] fabricated Pt–selenium (Pt–Se) nanozyme as potential candidates for selective colorimetric detection of Hg^{2+} with a LOD of 70 nmol L^{-1}. Zhao et al. [103] used poly (vinyl pyrrolidone) (PVP)-functionalized PtNPs nanozyme for the simultaneous determination of Hg^{2+} and Ag^{+} levels with LODs of 17.75 nmol L^{-1} and 9.75 nmol L^{-1}, respectively. Also, Kora and Rastogi [104] used biosynthesized PtNPs nanozymes for colorimetric detection of Hg^{2+} in tap and ground waters with LODs less than 16.9, and 47.3 nmol L^{-1}, respectively.

6.3. Other NPs

Hsu et al. [105] explored a fabricated bismuth oxy-iodide nanosystem as an efficient nano-network to selectively sense Hg^{2+} and Pb^{2+} down to nmol L^{-1} levels. Huang et al. [106] developed a bio-synthesized chitosan-functionalized molybdenum (IV) selenide nanozyme for the colorimetric detection of Hg^{2+}. The sensing system is based on the activating effect of Hg^{2+} on the synthesized nanozyme performance by the in-situ reduction of chitosan-adsorbed Hg^{2+}. The levels of Hg^{2+} can be selectively determined with a LOD of less than 5 nmol L^{-1}, using

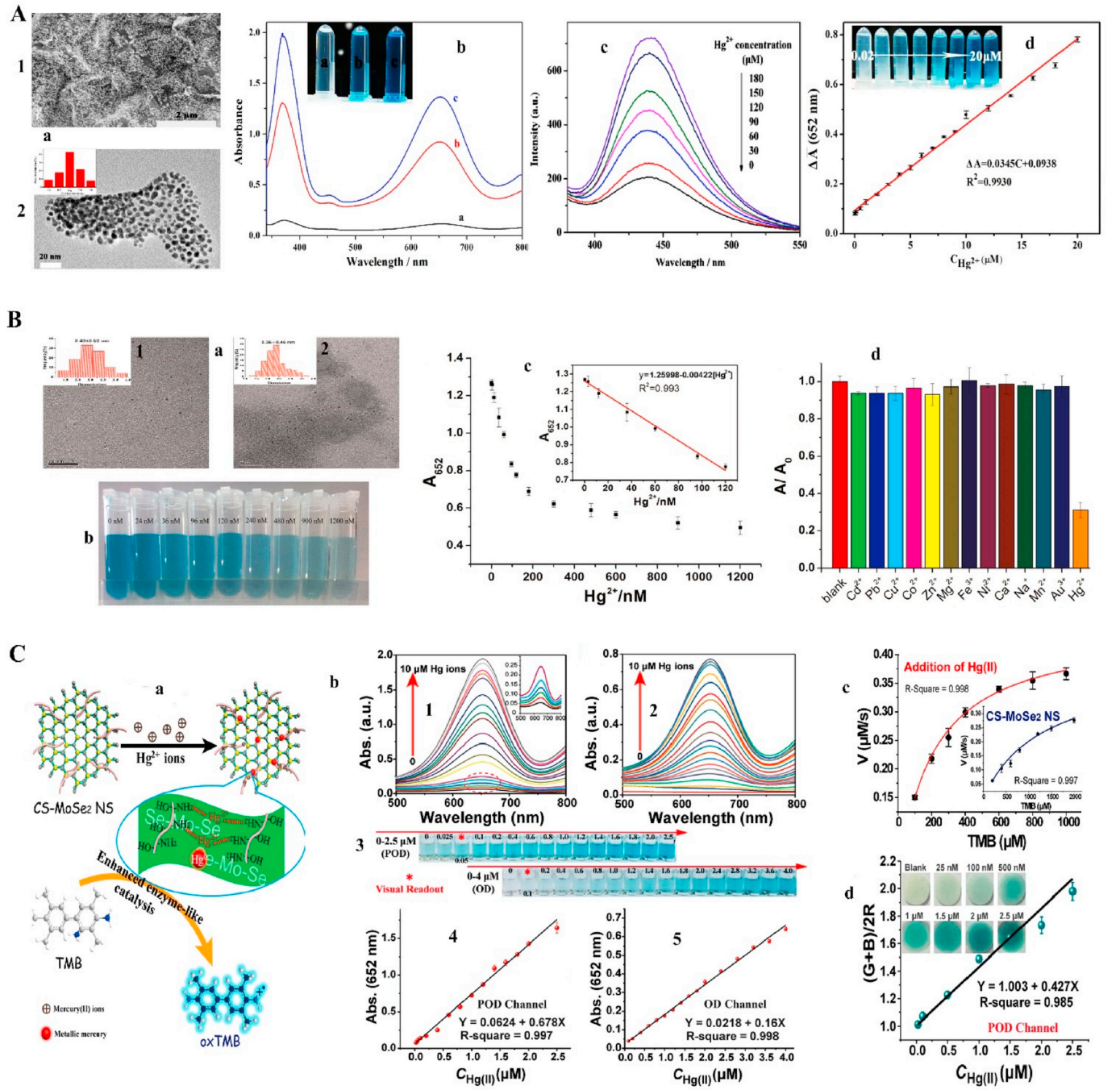

Fig. 4. A: Colorimetric determination of Hg^{2+} level in water based on peroxidase mimetic activity. a; Characterization of MoS_2–Au composites: (1) SEM, (2) TEM images. b; UV–vis absorption spectra of sodium acetate buffer solution containing 150 μM TMB and 50 mM H_2O_2: (a) No MoS_2–Au and Hg^{2+}, (b) in the presence of 20 μg/mL MoS_2–Au, (c) In the presence of 20 μg/mL MoS_2–Au and 50 μM Hg^{2+}. c; Effect of the Hg^{2+} level on the fluorescence intensity in the terephthalic acid-H_2O_2 system catalyzed by MoS_2–Au. d; Linear calibration plot for Hg^{2+} detection. The inset shows the color change of the chromogenic reaction in the presence of different levels of Hg^{2+} [91]. **B: BSA-stabilized Pt nanozyme for peroxidase mimetics and its application in colorimetric detection of Hg^{2+}.** a; TEM images of BSA–Pt reduced by DMAB at pH 7.0 (1), as well as reduced by $NaBH_4$ at pH7.0 (2). b; Photograph of the color progression with different levels of Hg^{2+} in the TMB–H_2O_2 reaction system (pH 4.0) catalyzed by BSA–Pt at 25 °C, c; Plots of the A652 values with the level of Hg^{2+}, d; the A652 values in the TMB–H_2O_2 reaction system (pH 4.0) catalyzed by BSA–Pt in the presence of Hg^{2+} (1 μM) or other ions (10 μM). The A_0 and A represent the A652 produced by BSA–Pt and BSA–Pt ion [98]. **C: Detection of Hg^{2+} based on a non-noble metal nanozyme.** a; Synthesis and characterization of CS-$MoSe_2$ NS. b; CS-$MoSe_2$ NS-based colorimetric Hg^{2+} assay. (1 and 2) UV absorption spectra of the reaction system that consisted of Hg^{2+}, 25 μg/mL CS-$MoSe_2$ NS, 20 mM H_2O^2, and 0.5 mM TMB and the reaction system that consisted of Hg^{2+}, 50 μg/mL CS-$MoSe_2$ NS, and 0.5 mM TMB, respectively. (3) Hg^{2+} level-related color changes of systems. (4 and 5) Linear relationships between the Hg^{2+} level and the absorbance of the reaction system obtained from panels 1 and 2, respectively. c; Kinetic plot of ν against TMB concentration before and after the addition of Hg^{2+} (10 μM) in the POD system. d; Plot of the (G + B)/2R value *vs* Hg^{2+} level in the POD channel. The images show the color of the test strip is varied with the Hg^{2+} level [106].

Table 5
Detection of Hg^{2+} using nanozymes.

Nanozyme	LOD for Hg^{2+}	Ref.
Cobalt sulfide	0.35 nmol L^{-1}	[137]
Cobalt sulfide/GO	14.23 mol L^{-1}	[20]
Cerium-based metal-organic framework	10.5 nmol L^{-1}	[138]
GO–Aunanohybrids	300 nmol L^{-1}	[139]
GO/Ag-cobalt/iron oxide (Fe2O4)	0.67 nmol L^{-1}	[140]
Iron oxide (Fe3O4)@zinc oxide (ZnO)	23 nmol L^{-1}	[141]
Fe3O4@zeolitic imidazolate framework (ZIF-67)	0.36 nmol L^{-1}	[142]
Fe3O4/Au/GO	0.15 nmol L^{-1}	[143]
Manganese oxide nanorods	0.08 μmol L^{-1}	[144]
Molybdenum disulfide nanosheets	0.5 μmol L^{-1}	[145]
Ag NPs	28 nmol L^{-1}	[146]
Ag@Ag3PO4	0.253 nmol L^{-1}	[147]

TMB as a colorimetric index. Furthermore, the integration of CS-$MoSe_2$ NS, with a smartphone, was tested for determination of Hg^{2+} level with a LOD of less than 10 nmol L^{-1} (Fig. 4C) [106]. This system demonstrated high selectivity and enhanced applicability in real samples, and showed a promising platform in the development of portable biocompatible nanozymes for the determination of Hg^{2+} level in a wider range of samples such as food, water and serum. Other nanozymes that are developed for the detection of Hg^{2+} are listed in Table 5.

7. Challenges and future perspective

It has been revealed that Hg^{2+} stimulates a wide range of adverse effects on human health. Therefore, it is crucial to assemble some well-developed platforms for determination of Hg^{2+} level as low as nmol L^{-1}, pmol L^{-1} or even fmol L^{-1} by different approaches. Several nanomaterials have been thoroughly assembled to mimic the conformation and activity of naturally existing enzymes. The development of nanozyme in determination of heavy metals levels has recently received a great deal of attention due to the sophisticated progress in the nanotechnology area. The nanozyme can be integrated with some monitoring systems such as well-developed software on portable phones to simplify its applicability. These systems can result in the development of advanced portable platforms for the determination of toxic ions and drugs levels in real samples. Optimizing the catalytic activity of nanozymes, the assembly of potential nanozymes based on different kinds of NPs with higher activity and other practical features are still required to develop promising nanozyme-based platforms in detection of heavy metals. Indeed, random trials of the enzyme-like functions of present nanomaterials should be oriented toward designing of enzyme-like performance based on those chemical compositions which are anticipated to accelerate enzymatic responses. Moreover, procedures to fabricate nanohybrids can be explored to solve the current crucial shortcoming of nanozymes showing low functional performance, by utilizing their synergistic impact to accelerate electron transfer between nanohybrid materials in the course of redox activity. Also, one of the most reported limitations of NPs as nanozymes is their adverse effect on the environment and biological systems. However, it seems that bio-inspired fabrication of NPs and their applications in the form of nanozymes may hold a great promise to synthesize safe and eco-friendly nanozymes. Because, plants and microbial systems can be used for bioremediation of Hg-containing samples [107,108]. This can be achieved by successfully dodging the utilization of harmful materials in classical chemical fabrication, through stimulating their applications in environmental treatments and therapeutic platforms. Finally, modification of the nanozyme surface may result in the selective and sensitive capability of nanomaterials to target potential substrates in the practical applications of nanozymes. With the abovementioned survey, it is anticipated that nanozymes will be extensively utilized in a number of implementations in the near future.

Taken together, future prospects of nanozymes for detection of Hg^{2+} in a wide range of samples such as food, industrial and medical compounds have gained a wide range of interest. Because, these types of diagnostic tools not only provide a high sensitivity and selectivity, but also they improve the diagnostic platforms demonstrating simple, portable and high repeatability features. Furthermore, the integration of nanozymes with a variety of portable smart devices such as mobile phones has led to an increased attention for their application in sensing-based analytical approaches. However, as mentioned above, many interdisciplinary activities are required to be well-developed to achieve a potential nanozyme-based detection system. For example, despite the rapid and accuracy of detection, the short-term stability of nanozymes should be considered in their various biological and environmental applications. Signaling amplification and LOD, which are addressed by the simultaneous utilization of different NPs are considered an important issues for future application of nanozymes. Finally, changing the phase of the sample may complicate the detection or sensing of the samples.

8. Conclusion

In this short review, we summarized recent progresses in expanding the determination of Hg^{2+} level in nature with a special focus on nanozymes. The nanozyme-stemmed approach is presently one of the promising methods used in sensing of heavy metals. However, the implementation of nanozymes to assemble a simple and eco-friendly strategy needs more assessments.

Declaration of competing interest

The authors declare no conflict of interest.

Acknowledgments

This research was made possible by the grants NPRP10-120-170-211 from Qatar National Research Fund (QNRF) under Qatar Foundation and GCC-2017-005 under the GCC collaborative research Program from Qatar University. The statements made herein are the sole responsibility of the authors.

References

[1] N. Pirrone, S. Cinnirella, X. Feng, R.B. Finkelman, H.R. Friedli, J. Leaner, R. Mason, A.B. Mukherjee, G.B. Stracher, D. Streets, Global mercury emissions to the atmosphere from anthropogenic and natural sources, Atmos. Chem. Phys. 10 (2010) 5951–5964.
[2] D.A. Rizzetti, F. Fernandez, S. Moreno, J.A.U. Ocio, F.M. Peçanha, G. Vera, D.V. Vassallo, M.M. Castro, G.A. Wiggers, Egg white hydrolysate promotes neuroprotection for neuropathic disorders induced by chronic exposure to low concentrations of mercury, Brain Res. 1646 (2016) 482–489.
[3] D.A. Rizzetti, Á. Martín, P. Corrales, F. Fernandez, M.R. Simões, F.M. Peçanha, D.V. Vassallo, M. Miguel, G.A. Wiggers, Egg white-derived peptides prevent cardiovascular disorders induced by mercury in rats: role of angiotensin-converting enzyme (ACE) and NADPH oxidase, Toxicol. Lett. (Shannon) 281 (2017) 158–174.
[4] D.A. Rizzetti, C.D.C. Altermann, C.S. Martinez, F.M. Peçanha, D.V. Vassallo, J.A. Uranga-Ocio, M.M. Castro, G.A. Wiggers, P.B. Mello-Carpes, Ameliorative effects of egg white hydrolysate on recognition memory impairments associated with chronic exposure to low mercury concentration, Neurochem. Int. 101 (2016) 30–37.
[5] W. Aragao, N. da Costa, N. Fagundes, M. Silva, S. Alves-Junior, J. Pinheiro, L. Amado, M. Crespo-López, C. Maia, R. Lima, Chronic exposure to inorganic mercury induces biochemical and morphological changes in the salivary glands of rats, Metall 9 (2017) 1271–1278.
[6] W.A.B. Aragão, F.B. Teixeira, N.C.F. Fagundes, R.M. Fernandes, L.M.P. Fernandes, M.C.F. da Silva, L.L. Amado, F.E.S. Sagica, E.H.C. Oliveira, M.E. Crespo-Lopez, Hippocampal dysfunction provoked by mercury chloride exposure: evaluation of cognitive impairment, oxidative stress, tissue injury and nature of cell death, Oxid. Med. Cell. Longev. 2018 (2018) 7878050.
[7] I.J.A. Belém-Filho, P.C. Ribera, A.L. Nascimento, A.R.Q. Gomes, R.R. Lima, M.E. Crespo-Lopez, M.C. Monteiro, E.A. Fontes-Júnior, M.O. Lima, C.S.F. Maia, Low doses of methylmercury intoxication solely or associated to ethanol binge drinking induce psychiatric-like disorders in adolescent female rats, Environ. Toxicol. Pharmacol. 60 (2018) 184–194.
[8] O. Onwuzuligbo, A.R. Hendricks, J. Hassler, K. Domanski, C. Goto, M.T. Wolf,

Mercury intoxication as a rare cause of membranous nephropathy in a child, Am. J. Kidney Dis. 72 (2018) 601–605.
[9] J.T. Salonen, K. Seppänen, K. Nyyssönen, H. Korpela, J. Kauhanen, M. Kantola, J. Tuomilehto, H. Esterbauer, F. Tatzber, R. Salonen, Intake of mercury from fish, lipid peroxidation, and the risk of myocardial infarction and coronary, cardiovascular, and any death in eastern Finnish men, Circulation 91 (1995) 645–655.
[10] T. Thompson, J. Fawell, S. Kunikane, D. Jackson, S. Appleyard, P. Callan, J. Bartram, P. Kingston, S. Water, W.H. Organization, Chemical Safety of Drinking Water: Assessing Priorities for Risk Management, (2007).
[11] J. Duan, J. Zhan, Recent developments on nanomaterials-based optical sensors for Hg2+ detection, Sci. China Mater. 58 (2015) 223–240.
[12] X. Liu, Y. Yao, Y. Ying, J. Ping, Recent advances in nanomaterial-enabled screen-printed electrochemical sensors for heavy metal detection, Trac. Trends Anal. Chem. 115 (2019) 187–202.
[13] N. Wang, M. Lin, H. Dai, H. Ma, Functionalized gold nanoparticles/reduced graphene oxide nanocomposites for ultrasensitive electrochemical sensing of mercury ions based on thymine–mercury–thymine structure, Biosens. Bioelectron. 79 (2016) 320–326.
[14] D. Rithesh Raj, S. Prasanth, T.V. Vineeshkumar, C. Sudarsanakumar, Surface Plasmon Resonance based fiber optic sensor for mercury detection using gold nanoparticles PVA hybrid, Optic Commun. 367 (2016) 102–107.
[15] Y. Ding, S. Wang, J. Li, L. Chen, Nanomaterial-based optical sensors for mercury ions, Trac. Trends Anal. Chem. 82 (2016) 175–190.
[16] Y.Q. Huang, S. Fu, Y.S. Wang, J.H. Xue, X.L. Xiao, S.H. Chen, B. Zhou, Protamine-gold nanoclusters as peroxidase mimics and the selective enhancement of their activity by mercury ions for highly sensitive colorimetric assay of Hg(II), Anal. Bioanal. Chem. 410 (2018) 7385–7394.
[17] Y. Liu, D. Ding, Y. Zhen, R. Guo, Amino acid-mediated 'turn-off/turn-on' nanozyme activity of gold nanoclusters for sensitive and selective detection of copper ions and histidine, Biosens. Bioelectron. 92 (2017) 140–146.
[18] R. Zeng, Z. Luo, L. Zhang, D. Tang, Platinum nanozyme-catalyzed gas generation for pressure-based bioassay using polyaniline nanowires-functionalized graphene oxide framework, Anal. Chem. 90 (2018) 12299–12306.
[19] C.-F. Peng, Y.-Y. Zhang, L.-Y. Wang, Z.-Y. Jin, G. Shao, Colorimetric assay for the simultaneous detection of Hg2+ and Ag+ based on inhibiting the peroxidase-like activity of core–shell Au@Pt nanoparticles, Anal. Methods 9 (2017) 4363–4370.
[20] P. Borthakur, G. Darabdhara, M.R. Das, R. Boukherroub, S. Szunerits, Solvothermal synthesis of CoS/reduced porous graphene oxide nanocomposite for selective colorimetric detection of Hg(II) ion in aqueous medium, Sensor. Actuator. B Chem. 244 (2017) 684–692.
[21] S. Zhang, D. Zhang, X. Zhang, D. Shang, Z. Xue, D. Shan, X. Lu, Ultratrace naked-eye colorimetric detection of Hg(2+) in wastewater and serum utilizing mercury-stimulated peroxidase mimetic activity of reduced graphene oxide-PEI-Pd nanohybrids, Anal. Chem. 89 (2017) 3538–3544.
[22] M. Sharifi, S.H. Hosseinali, A.A. Saboury, E. Szegezdi, M. Falahati, Involvement of planned cell death of necroptosis in cancer treatment by nanomaterials: recent advances and future perspectives, J. Contr. Release 299 (2019) 121–137.
[23] Q. Shi, N. Sun, H. Kou, H. Wang, H. Zhao, Chronic effects of mercury on Bufo gargarizans larvae: thyroid disruption, liver damage, oxidative stress and lipid metabolism disorder, Ecotoxicol. Environ. Saf. 164 (2018) 500–509.
[24] G. Gallego-Vinas, F. Ballester, S. Llop, Chronic mercury exposure and blood pressure in children and adolescents: a systematic review, Environ. Sci. Pollut. Res. Int. 26 (2019) 2238–2252.
[25] R.A. Bernhoft, Mercury toxicity and treatment: a review of the literature, J. Environ. Pub. Health 2012 (2012).
[26] F. Zahir, S.J. Rizwi, S.K. Haq, R.H. Khan, Low dose mercury toxicity and human health, Environ. Toxicol. Pharmacol. 20 (2005) 351–360.
[27] I.A. Al-Saleh, Health implications of mercury exposure in children, Int. J. Environ. Health 3 (2009) 22–57.
[28] C. Després, A. Beuter, F. Richer, K. Poitras, A. Veilleux, P. Ayotte, E. Dewailly, D. Saint-Amour, G. Muckle, Neuromotor functions in Inuit preschool children exposed to Pb, PCBs, and Hg, Neurotoxicol. Teratol. 27 (2005) 245–257.
[29] F. Debes, E. Budtz-Jørgensen, P. Weihe, R.F. White, P. Grandjean, Impact of prenatal methylmercury exposure on neurobehavioral function at age 14 years, Neurotoxicol. Teratol. 28 (2006) 536–547.
[30] V.L. Cariccio, A. Samà, P. Bramanti, E. Mazzon, Mercury involvement in neuronal damage and in neurodegenerative diseases, Biol. Trace Elem. Res. 187 (2019) 341–356.
[31] R. Pamphlett, S.K. Jew, Inorganic mercury in human astrocytes, oligodendrocytes, corticomotoneurons and the locus ceruleus: implications for multiple sclerosis, neurodegenerative disorders and gliomas, Biometals 31 (2018) 807–819.
[32] P.D. Pigatto, A. Costa, G. Guzzi, Are mercury and Alzheimer's disease linked? Sci. Total Environ. 613 (2018) 1579–1580.
[33] M.R. Carratù, A. Signorile, Methyl mercury injury to CNS: mitochondria at the core of the matter, Open Acc. Toxicol 1 (2015) 1–6.
[34] R. Ynalvez, J. Gutierrez, H. Gonzalez-Cantu, Mini-review: toxicity of mercury as a consequence of enzyme alteration, Biometals 29 (2016) 781–788.
[35] A.A. dos Santos, C. López-Granero, M. Farina, J.B. Rocha, A.B. Bowman, M. Aschner, Oxidative stress, caspase-3 activation and cleavage of ROCK-1 play an essential role in MeHg-induced cell death in primary astroglial cells, Food Chem. Toxicol. 113 (2018) 328–336.
[36] F.B. Teixeira, A.C. de Oliveira, L.K. Leão, N.C. Fagundes, R.M. Fernandes, L.M. Fernandes, M.C. da Silva, L.L. Amado, F.E. Sagica, E.H. de Oliveira, Exposure to inorganic mercury causes oxidative stress, cell death, and functional deficits in the motor cortex, Front. Mol. Neurosci. 11 (2018).
[37] L.N. da Silva Santana, L.O. Bittencourt, P.C. Nascimento, R.M. Fernandes, F.B. Teixeira, L.M.P. Fernandes, M.C.F. Silva, L.S. Nogueira, L.L. Amado, M.E. Crespo-Lopez, Low doses of methylmercury exposure during adulthood in rats display oxidative stress, neurodegeneration in the motor cortex and lead to impairment of motor skills, J. Trace Elem. Med. Biol. 51 (2019) 19–27.
[38] M. Simões, B. Azevedo, J. Fiorim, D. Jr Freire, E. Covre, D. Vassallo, L. Dos Santos, Chronic mercury exposure impairs the sympathovagal control of the rat heart, Clin. Exp. Pharmacol. Physiol. 43 (2016) 1038–1045.
[39] M.O. Gribble, A. Cheng, R.D. Berger, L. Rosman, E. Guallar, Mercury exposure and heart rate variability: a systematic review, Curr. Environ. Health Rep. 2 (2015) 304–314.
[40] V.A. Oliveira, G. Favero, A. Stacchiotti, L. Giugno, B. Buffoli, C.S. de Oliveira, A. Lavazza, M. Albanese, L.F. Rodella, M.E. Pereira, Acute mercury exposition of virgin, pregnant, and lactating rats: histopathological kidney and liver evaluations, Environ. Toxicol. 32 (2017) 1500–1512.
[41] A. Hounkpatin, C. Roch, M. Senou, L. Dovonon, G. Chibuisi, S.G. Alimba, J.M. Gnonlonfoun, I. Glitho, Protective effects of vitamin C on kidney, liver and brain: a study in wistar rats intoxicated with mercury, Ann. UP Série Sci. Nat. Agron. 7 (2017) 168–177.
[42] M.-R. Lee, Y.-H. Lim, B.-E. Lee, Y.-C. Hong, Blood mercury concentrations are associated with decline in liver function in an elderly population: a panel study, Environ. Health 16 (2017) 17.
[43] M.H. Hazelhoff, A.M. Torres, Gender differences in mercury-induced hepatotoxicity: potential mechanisms, Chemosphere 202 (2018) 330–338.
[44] Y.B. Ho, N.H. Abdullah, H. Hamsan, E.S.S. Tan, Mercury contamination in facial skin lightning creams and its health risks to user, Regul. Toxicol. Pharmacol. 88 (2017) 72–76.
[45] C.S. Martinez, F.M. Pecanha, D.S. Brum, F.W. Santos, J.L. Franco, A.P.P. Zemolin, J.A. Anselmo-Franci, F.B. Junior, M.J. Alonso, M. Salaices, D.V. Vassallo, F.G. Leivas, G.A. Wiggers, Reproductive dysfunction after mercury exposure at low levels: evidence for a role of glutathione peroxidase (GPx) 1 and GPx4 in male rats, Reprod. Fertil. Dev. 29 (2017) 1803–1812.
[46] M.C. Henriques, S. Loureiro, M. Fardilha, M.T. Herdeiro, Exposure to mercury and human reproductive health: a systematic review, Reprod. Toxicol. 85 (2019) 93–103.
[47] X.F. Hu, K. Singh, H.M. Chan, Mercury exposure, blood pressure, and hypertension: a systematic review and dose-response meta-analysis, Environ. Health Perspect. 126 (2018) 076002.
[48] R. Zefferino, C. Piccoli, N. Ricciardi, R. Scrima, N. Capitanio, Possible mechanisms of mercury toxicity and cancer promotion: involvement of gap junction intercellular communications and inflammatory cytokines, Oxid. Med. Cell. Longev. (2017) 2017.
[49] Y. Fang, Y. Pan, P. Li, M. Xue, F. Pei, W. Yang, N. Ma, Q. Hu, Simultaneous determination of arsenic and mercury species in rice by ion-pairing reversed phase chromatography with inductively coupled plasma mass spectrometry, Food Chem. 213 (2016) 609–615.
[50] S. Ma, M. He, B. Chen, W. Deng, Q. Zheng, B. Hu, Magnetic solid phase extraction coupled with inductively coupled plasma mass spectrometry for the speciation of mercury in environmental water and human hair samples, Talanta 146 (2016) 93–99.
[51] N. Panichev, S. Panicheva, Determination of total mercury in fish and sea products by direct thermal decomposition atomic absorption spectrometry, Food Chem. 166 (2015) 432–441.
[52] I.L. Almeida, M.D. Oliveira, J.B. Silva, N.M. Coelho, Suitable extraction of soils and sediments for mercury species and determination combined with the cold vapor generation atomic absorption spectrometry technique, Microchem. J. 124 (2016) 326–330.
[53] R. Zhang, M. Peng, C. Zheng, K. Xu, X. Hou, Application of flow injection–green chemical vapor generation–atomic fluorescence spectrometry to ultrasensitive mercury speciation analysis of water and biological samples, Microchem. J. 127 (2016) 62–67.
[54] Q. Zou, X. Li, T. Xue, J. Zheng, Q. Su, SERS detection of mercury (II)/lead (II): a new class of DNA logic gates, Talanta 195 (2019) 497–505.
[55] F. Ma, Y. Chen, Y. Zhu, J. Liu, Electrogenerated chemiluminescence biosensor for detection of mercury (II) ion via target-triggered manipulation of DNA three-way junctions, Talanta 194 (2019) 114–118.
[56] H.J. Chun, S. Kim, Y.D. Han, D.W. Kim, K.R. Kim, H.S. Kim, J.H. Kim, H.C. Yoon, Water-soluble mercury ion sensing based on the thymine-Hg(2+)-thymine base pair using retroreflective Janus particle as an optical signaling probe, Biosens. Bioelectron. 104 (2018) 138–144.
[57] N. Xia, F. Feng, C. Liu, R. Li, W. Xiang, H. Shi, L. Gao, The detection of mercury ion using DNA as sensors based on fluorescence resonance energy transfer, Talanta 192 (2019) 500–507.
[58] X. Cui, L. Zhu, J. Wu, Y. Hou, P. Wang, Z. Wang, M. Yang, A fluorescent biosensor based on carbon dots-labeled oligodeoxyribonucleotide and graphene oxide for mercury (II) detection, Biosens. Bioelectron. 63 (2015) 506–512.
[59] D.N. Wordofa, P. Ramnani, T.T. Tran, A. Mulchandani, An oligonucleotide-functionalized carbon nanotube chemiresistor for sensitive detection of mercury in saliva, Analyst 141 (2016) 2756–2760.
[60] A.G. Memon, X. Zhou, J. Liu, R. Wang, L. Liu, B. Yu, M. He, H. Shi, Utilization of unmodified gold nanoparticles for label-free detection of mercury (II): insight into rational design of mercury-specific oligonucleotides, J. Hazard Mater. 321 (2017) 417–423.
[61] K. Asadpour-Zeynali, R. Amini, A novel voltammetric sensor for mercury(II) based on mercaptocarboxylic acid intercalated layered double hydroxide nanoparticles modified electrode, Sensor. Actuator. B Chem. 246 (2017) 961–968.
[62] N.R. Devi, M. Sasidharan, A.K. Sundramoorthy, Gold nanoparticles-thiol-

functionalized reduced graphene oxide coated electrochemical sensor system for selective detection of mercury ion, J. Electrochem. Soc. 165 (2018) B3046–B3053.
[63] P. Sharma, M. Mourya, D. Choudhary, M. Goswami, I. Kundu, M.P. Dobhal, C.S.P. Tripathi, D. Guin, Thiol terminated chitosan capped silver nanoparticles for sensitive and selective detection of mercury (II) ions in water, Sensor. Actuator. B Chem. 268 (2018) 310–318.
[64] Y. Guo, Z. Wang, W. Qu, H. Shao, X. Jiang, Colorimetric detection of mercury, lead and copper ions simultaneously using protein-functionalized gold nanoparticles, Biosens. Bioelectron. 26 (2011) 4064–4069.
[65] L. Feng, J. Sha, Y. He, S. Chen, B. Liu, H. Zhang, C. Lü, Conjugated polymer and spirolactam rhodamine-B derivative co-functionalized mesoporous silica nanoparticles as the scaffold for the FRET-based ratiometric sensing of mercury (II) ions, Microporous Mesoporous Mater. 208 (2015) 113–119.
[66] Z. Chen, C. Zhang, Y. Tan, T. Zhou, H. Ma, C. Wan, Y. Lin, K. Li, Chitosan-functionalized gold nanoparticles for colorimetric detection of mercury ions based on chelation-induced aggregation, Microchim. Acta 182 (2015) 611–616.
[67] K.B. Narayanan, S.S. Han, Highly selective and quantitative colorimetric detection of mercury(II) ions by carrageenan-functionalized Ag/AgCl nanoparticles, Carbohydr. Polym. 160 (2017) 90–96.
[68] H. Tianyu, Y. Xu, N. Weidan, S. Xingguang, Aptamer-based aggregation assay for mercury(II) using gold nanoparticles and fluorescent CdTe quantum dots, Microchim. Acta 183 (2016) 2131–2137.
[69] Y. Lu, J. Zhong, G. Yao, Q. Huang, A label-free SERS approach to quantitative and selective detection of mercury (II) based on DNA aptamer-modified SiO2@Au core/shell nanoparticles, Sensor. Actuator. B Chem. 258 (2018) 365–372.
[70] Y. Liu, Q. Ouyang, H. Li, M. Chen, Z. Zhang, Q. Chen, Turn-on fluoresence sensor for Hg(2+) in food based on FRET between aptamers-functionalized upconversion nanoparticles and gold nanoparticles, J. Agric. Food Chem. 66 (2018) 6188–6195.
[71] L. Duan, X. Song, H. Sun, S. Yang, F. Liao, O-Phenylenediamine-Cysteine nanosphere having conjugated structures: a highly selective fluorescent probe for mercury ion, J. Adv. Nano. 1 (2016) 21–32.
[72] X. Liu, D. Huang, C. Lai, G. Zeng, L. Qin, H. Wang, H. Yi, B. Li, S. Liu, M. Zhang, R. Deng, Y. Fu, L. Li, W. Xue, S. Chen, Recent advances in covalent organic frameworks (COFs) as a smart sensing material, Chem. Soc. Rev. 48 (2019) 5266–5302.
[73] O.M. Yaghi, M.J. Kalmutzki, C.S. Diercks, Introduction to Reticular Chemistry: Metal-Organic Frameworks and Covalent Organic Frameworks, John Wiley & Sons2019.
[74] W. Li, Y. Li, H.-L. Qian, X. Zhao, C.-X. Yang, X.-P. Yan, Fabrication of a covalent organic framework and its gold nanoparticle hybrids as stable mimetic peroxidase for sensitive and selective colorimetric detection of mercury in water samples, Talanta 204 (2019) 224–228.
[75] Y. He, X. Wang, K. Wang, L. Wang, A triarylamine-based fluorescent covalent organic framework for efficient detection and removal of Mercury (II) ion, Dyes Pigments 173 (2020) 107880.
[76] L. Guo, Y. Song, K. Cai, L. Wang, "On-off" ratiometric fluorescent detection of Hg2+ based on N-doped carbon dots-rhodamine B@TAPT-DHTA-COF, Spectrochim. Acta 227 (2020) 117703.
[77] M. Sharifi, S.H. Hosseinali, P. Yousefvand, A. Salihi, M.S. Shekha, F.M. Aziz, A. JouyaTalaei, A. Hasan, M. Falahati, Gold nanozyme: biosensing and therapeutic activities, Mater. Sci. Eng. C 108 (2020) 110422.
[78] M. Sharifi, K. Faryabi, A.J. Talaei, M.S. Shekha, M. Ale-Ebrahim, A. Salihi, N.M.Q. Nanakali, F.M. Aziz, B. Rasti, A. Hasan, M. Falahati, Antioxidant properties of gold nanozyme: a review, J. Mol. Liq. (2019) 112004.
[79] A.M. Pyle, Ribozymes: a distinct class of metalloenzymes, Science 261 (1993) 709–714.
[80] G.A. Nevinsky, T.G. Kanyshkova, V.N. Buneva, Natural catalytic antibodies (abzymes) in normalcy and pathology, Biochemistry 65 (2000) 1245–1255.
[81] I. Willner, B. Shlyahovsky, M. Zayats, B. Willner, DNAzymes for sensing, nanobiotechnology and logic gate applications, Chem. Soc. Rev. 37 (2008) 1153–1165.
[82] F. Attar, M.G. Shahpar, B. Rasti, M. Sharifi, A.A. Saboury, S.M. Rezayat, M. Falahati, Nanozymes with intrinsic peroxidase-like activities, J. Mol. Liq. 278 (2019) 130–144.
[83] D. Zhou, K. Zeng, M. Yang, Gold nanoparticle-loaded hollow Prussian Blue nanoparticles with peroxidase-like activity for colorimetric determination of L-lactic acid, Microchim. Acta 186 (2019) 121.
[84] K.Y. Wang, S.J. Bu, C.J. Ju, Y. Han, C.Y. Ma, W.S. Liu, Z.Y. Li, C.T. Li, J.Y. Wan, Disposable syringe-based visual immunotest for pathogenic bacteria based on the catalase mimicking activity of platinum nanoparticle-concanavalin A hybrid nanoflowers, Microchim. Acta 186 (2019) 57.
[85] P. Pengo, S. Polizzi, L. Pasquato, P. Scrimin, Carboxylate – Imidazole cooperativity in dipeptide-functionalized gold nanoparticles with esterase-like activity, J. Am. Chem. Soc. 127 (2005) 1616–1617.
[86] S. Iravani, H. Korbekandi, S.V. Mirmohammadi, B. Zolfaghari, Synthesis of silver nanoparticles: chemical, physical and biological methods, Res. Pharm. Sci. 9 (2014) 385–406.
[87] Y. Lv, M. Ma, Y. Huang, Y. Xia, Carbon dot nanozymes: how to Be close to natural enzymes, Chem. Eur. 25 (2019) 954–960.
[88] B. Xu, H. Wang, W. Wang, L. Gao, S. Li, X. Pan, H. Wang, H. Yang, X. Meng, Q. Wu, L. Zheng, S. Chen, X. Shi, K. Fan, X. Yan, H. Liu, A single-atom nanozyme for wound disinfection applications, Angew. Chem. 131 (2019) 4965–4970.
[89] C. Peng, M.Y. Hua, N.S. Li, Y.P. Hsu, Y.T. Chen, C.K. Chuang, S.T. Pang, H.W. Yang, A colorimetric immunosensor based on self-linkable dual-nanozyme for ultrasensitive bladder cancer diagnosis and prognosis monitoring, Biosens. Bioelectron. 126 (2019) 581–589.
[90] M. Yin, Z. Duan, C. Zhang, L. Feng, Y. Wan, Y. Cai, H. Liu, S. Li, H. Wang, A visualized colorimetric detection strategy for heparin in serum using a metal-free polymer nanozyme, Microchem. J. 145 (2019) 864–871.
[91] C. Ma, Y. Ma, Y. Sun, Y. Lu, E. Tian, J. Lan, J. Li, W. Ye, H. Zhang, Colorimetric determination of Hg(2+) in environmental water based on the Hg(2+)-stimulated peroxidase mimetic activity of MoS2-Au composites, J. Colloid Interface Sci. 537 (2019) 554–561.
[92] K.N. Han, J.S. Choi, J. Kwon, Gold nanozyme-based paper chip for colorimetric detection of mercury ions, Sci. Rep. 7 (2017) 2806.
[93] Y. Zhao, H. Qiang, Z. Chen, Colorimetric determination of Hg (II) based on a visually detectable signal amplification induced by a Cu@ Au-Hg trimetallic amalgam with peroxidase-like activity, Microchim. Acta 184 (2017) 107–115.
[94] N. Zohora, D. Kumar, M. Yazdani, V.M. Rotello, R. Ramanathan, V. Bansal, Rapid colorimetric detection of mercury using biosynthesized gold nanoparticles, Colloid. Surface. 532 (2017) 451–457.
[95] C. Jiang, Z. Li, Y. Wu, W. Guo, J. Wang, Q. Jiang, Colorimetric detection of Hg2+ based on enhancement of peroxidase-like activity of chitosan-gold nanoparticles, Bull. Kor. Chem. Soc. 39 (2018) 625–630.
[96] Y.W. Wang, Q. Liu, L. Wang, S. Tang, H.H. Yang, H. Song, A colorimetric mercury (II) assay based on the Hg(II)-stimulated peroxidase mimicking activity of a nanocomposite prepared from graphitic carbon nitride and gold nanoparticles, Mikrochim. Acta 186 (2018) 7.
[97] W. Li, B. Chen, H. Zhang, Y. Sun, J. Wang, J. Zhang, Y. Fu, BSA-stabilized Pt nanozyme for peroxidase mimetics and its application on colorimetric detection of mercury(II) ions, Biosens. Bioelectron. 66 (2015) 251–258.
[98] Y. Zhao, H. Qiang, Z. Chen, Colorimetric determination of Hg(II) based on a visually detectable signal amplification induced by a Cu@Au-Hg trimetallic amalgam with peroxidase-like activity, Microchim. Acta 184 (2017) 107–115.
[99] Y. Zhou, Z. Ma, Fluorescent and colorimetric dual detection of mercury (II) by H2O2 oxidation of o-phenylenediamine using Pt nanoparticles as the catalyst, Sensor. Actuator. B Chem. 249 (2017) 53–58.
[100] H. Li, H. Liu, J. Zhang, Y. Cheng, C. Zhang, X. Fei, Y. Xian, Platinum nanoparticle encapsulated metal–organic frameworks for colorimetric measurement and facile removal of mercury(II), ACS Appl. Mater. Interfaces 9 (2017) 40716–40725.
[101] Y.W. Wang, L. Wang, F. An, H. Xu, Z. Yin, S. Tang, H.H. Yang, H. Song, Graphitic carbon nitride supported platinum nanocomposites for rapid and sensitive colorimetric detection of mercury ions, Anal. Chim. Acta 980 (2017) 72–78.
[102] L. Guo, L. Mao, K. Huang, H. Liu, Pt–Se nanostructures with oxidase-like activity and their application in a selective colorimetric assay for mercury(II), J. Mater. Sci. 52 (2017) 10738–10750.
[103] Y. Zhao, X. Yang, L. Cui, Y. Sun, Q. Song, PVP-capped Pt NPs-depended catalytic nanoprobe for the simultaneous detection of Hg2+ and Ag+, Dyes Pigments 150 (2018) 21–26.
[104] A.J. Kora, L. Rastogi, Peroxidase activity of biogenic platinum nanoparticles: a colorimetric probe towards selective detection of mercuric ions in water samples, Sensor. Actuator. B Chem. 254 (2018) 690–700.
[105] C.-L. Hsu, C.-W. Lien, S.G. Harroun, R. Ravindranath, H.-T. Chang, J.-Y. Mao, C.-C. Huang, Metal-deposited bismuth oxyiodide nanonetworks with tunable enzyme-like activity: sensing of mercury and lead ions, Mater. Chem. Front. 1 (2017) 893–899.
[106] L. Huang, Q. Zhu, J. Zhu, L. Luo, S. Pu, W. Zhang, W. Zhu, J. Sun, J. Wang, Portable colorimetric detection of mercury(II) based on a non-noble metal nanozyme with tunable activity, Inorg. Chem. 58 (2019) 1638–1646.
[107] O.B. Ojuederie, O.O. Babalola, Microbial and plant-assisted bioremediation of heavy metal polluted environments: a review, Int. J. Environ. Res. Publ. Health 14 (2017) 1504.
[108] M.M. Naguib, A.O. El-Gendy, A.S. Khairalla, Microbial diversity of mer operon genes and their potential rules in mercury bioremediation and resistance, Open Biotechnol. J. 12 (2018).
[109] C.-H. Yao, S.-J. Jiang, A. Sahayam, Y.-L. Huang, Speciation of mercury in fish oils using liquid chromatography inductively coupled plasma mass spectrometry, Microchem. J. 133 (2017) 556–560.
[110] E.J. Drobyshev, N.D. Solovyev, N.B. Ivanenko, M.Y. Kombarova, A.A. Ganeev, Trace element biomonitoring in hair of school children from a polluted area by sector field inductively coupled plasma mass spectrometry, J. Trace Elem. Med. Biol. 39 (2017) 14–20.
[111] S. Zhu, B. Chen, M. He, T. Huang, B. Hu, Speciation of mercury in water and fish samples by HPLC-ICP-MS after magnetic solid phase extraction, Talanta 171 (2017) 213–219.
[112] B. Song, H. He, L. Chen, S. Yang, Y. Yongguang, Y. Li, Speciation of mercury in microalgae by isotope dilution-inductively coupled plasma mass spectrometry, Anal. Lett. 50 (2017) 2161–2176.
[113] N. Khan, N. Jamila, Y. MiDang, C.M. Lee, Y.M. Park, G.H. Lee, C.M. Ja, K.S. Kim, Elemental analysis of stone fruits by inductively coupled plasma mass spectrometry and direct mercury analysis, Anal. Lett. 50 (2017) 2426–2446.
[114] H. Cheng, X. Chen, L. Shen, Y. Wang, Z. Xu, J. Liu, Ion-pairing reversed-phase chromatography coupled to inductively coupled plasma mass spectrometry as a tool to determine mercurial species in freshwater fish, J. Chromatogr. A 1531 (2018) 104–111.
[115] H. Cheng, W. Zhang, Y. Wang, J. Liu, Interfacing nanoliter liquid chromatography and inductively coupled plasma mass spectrometry with an in-column high-pressure nebulizer for mercury speciation, J. Chromatogr. A 1575 (2018) 59–65.
[116] W. Wohlmann, V.M. Neves, G.M. Heidrich, J.S. Silva, A.B. da Costa, J.N. Paniz, V.L. Dressler, Development of an electrothermal vaporizer for direct mercury determination in soil by inductively-coupled plasma mass spectrometry, Spectrochim. Acta B 149 (2018) 222–228.
[117] M.d.L. Potes, L. Kolling, A. de Jesus, M.B. Dessuy, M.G.R. Vale, M.M. da Silva,

Determination of mercury in fish by photochemical vapor generation graphite furnace atomic absorption spectrometry, Anal. Methods 8 (2016) 8165–8172.
[118] A. Sabouri, S. Nouroozi, Direct determination of total mercury in urine samples using flow injection catalytic cold vapor atomic absorption spectrometry (FI-CCV-AAS), RSC Adv.s 6 (2016) 80354–80360.
[119] E. Yavuz, Ş. Tokalıoğlu, Ş. Patat, Magnetic dispersive solid phase extraction with graphene/ZnFe2O4 nanocomposite adsorbent for the sensitive determination of mercury in water and fish samples by cold vapor atomic absorption spectrometry, Microchem. J. 142 (2018) 85–93.
[120] O. Caylak, S.G. Elci, A. Hol, A. Akdogan, U. Divrikli, L. Elci, Use of an aminated Amberlite XAD-4 column coupled to flow injection cold vapour generation atomic absorption spectrometry for mercury speciation in water and fish tissue samples, Food Chem. 274 (2019) 487–493.
[121] M. Senila, E. Covaci, O. Cadar, M. Ponta, M. Frentiu, T. Frentiu, Mercury speciation in fish tissue by eco-scale thermal decomposition atomic absorption spectrometry: method validation and risk exposure to methylmercury, Chem. Pap. 72 (2018) 441–448.
[122] Y. Zhang, M. Miró, S.D. Kolev, A novel on-line organic mercury digestion method combined with atomic fluorescence spectrometry for automatic mercury speciation, Talanta 189 (2018) 220–224.
[123] P. Hu, X. Wang, L. Yang, H. Yang, Y. Tang, H. Luo, X. Xiong, X. Jiang, K. Huang, Speciation of mercury by hydride generation ultraviolet atomization-atomic fluorescence spectrometry without chromatographic separation, Microchem. J. 143 (2018) 228–233.
[124] J. Savoie, R. St-Louis, M. Clément, Facilitating local analysis in northern regions: microwave plasma-atomic emission spectrometry for mercury determination in wild Atlantic salmon, Int. J. Environ. Anal. Chem. 98 (2018) 582–591.
[125] R.F. Huang, H.X. Liu, Q.Q. Gai, G.J. Liu, Z. Wei, A facile and sensitive electrochemiluminescence biosensor for Hg2+ analysis based on a dual-function oligonucleotide probe, Biosens. Bioelectron. 71 (2015) 194–199.
[126] Y.L. Huang, Z.F. Gao, J. Jia, H.Q. Luo, N.B. Li, A label-free electrochemical sensor for detection of mercury(II) ions based on the direct growth of guanine nanowire, J. Hazard Mater. 308 (2016) 173–178.
[127] Y. Wei, G. Shangguan, J. Yang, K. Zhang, An ecological study of nano-graphite as A cheap, effective fluorescent sensing platform for mercury (II) ion detection in aqueous solutions, Ekoloji 27 (2018) 2083–2087.
[128] Q. Zhang, Y. Ni, S. Kokot, The use of DNA self-assembled gold nano-rods for novel analysis of lead and/or mercury in drinking water, Anal. Methods 7 (2015) 4514–4520.
[129] H. Yang, S.-B. Ye, Y. Fu, W. Zhang, F. Xie, L. Gong, P.-P. Fang, J. Chen, Y. Tong, A simple and highly sensitive thymine sensor for mercury ion detection based on surface enhanced Raman spectroscopy and the mechanism study, Nanomaterials 7 (2017) 192.
[130] Y. Zhang, G.M. Zeng, L. Tang, J. Chen, Y. Zhu, X.X. He, Y. He, Electrochemical sensor based on electrodeposited graphene-Au modified electrode and nanoAu carrier amplified signal strategy for attomolar mercury detection, Anal. Chem. 87 (2015) 989–996.
[131] Y. Chen, L. Wu, Y. Chen, N. Bi, X. Zheng, H. Qi, M. Qin, X. Liao, H. Zhang, Y. Tian, Determination of mercury(II) by surface-enhanced Raman scattering spectroscopy based on thiol-functionalized silver nanoparticles, Microchim. Acta 177 (2012) 341–348.
[132] Z. Chen, C. Zhang, H. Ma, T. Zhou, B. Jiang, M. Chen, X. Chen, A non-aggregation spectrometric determination for mercury ions based on gold nanoparticles and thiocyanuric acid, Talanta 134 (2015) 603–606.
[133] K. Tyszczuk-Rotko, I. Sadok, M. Barczak, Thiol-functionalized polysiloxanes modified by lead nanoparticles: synthesis, characterization and application for determination of trace concentrations of mercury(II), Microporous Mesoporous Mater. 230 (2016) 109–117.
[134] A. Gupta, A. Chaudhary, P. Mehta, C. Dwivedi, S. Khan, N.C. Verma, C.K. Nandi, Nitrogen-doped, thiol-functionalized carbon dots for ultrasensitive Hg(ii) detection, Chem. Commun. 51 (2015) 10750–10753.
[135] K. Daware, R. Shinde, R.S. Kalubarme, M. Kasture, A. Pandey, C. Terashima, S.W. Gosavi, Development of optical sensing probe for Hg(II) ions detection in ground water using Au, Hexanedithiol and Rhodamine B nanocomposite system, Sensor. Actuator. B Chem. 265 (2018) 547–555.
[136] A. Rajeshwari, D. Karthiga, N. Chandrasekaran, A. Mukherjee, Anti-aggregation-based spectrometric detection of Hg(II) at physiological pH using gold nanorods, Mat. Sci. Eng. C. Mater. 67 (2016) 711–716.
[137] H. Yang, J. Zha, P. Zhang, Y. Xiong, L. Su, F. Ye, Sphere-like CoS with nanostructures as peroxidase mimics for colorimetric determination of H2O2 and mercury ions, RSC Adv. 6 (2016) 66963–66970.
[138] C. Wang, G. Tang, H. Tan, Colorimetric determination of mercury(II) via the inhibition by ssDNA of the oxidase-like activity of a mixed valence state cerium-based metal-organic framework, Mikrochim. Acta 185 (2018) 475.
[139] X. Chen, N. Zhai, J.H. Snyder, Q. Chen, P. Liu, L. Jin, Q. Zheng, F. Lin, J. Hu, H. Zhou, Colorimetric detection of Hg2+ and Pb2+ based on peroxidase-like activity of graphene oxide–gold nanohybrids, Anal. Methods 7 (2015) 1951–1957.
[140] Y. Guo, Y. Tao, X. Ma, J. Jin, S. Wen, W. Ji, W. Song, B. Zhao, Y. Ozaki, A dual colorimetric and SERS detection of Hg2+ based on the stimulus of intrinsic oxidase-like catalytic activity of Ag-CoFe2O4/reduced graphene oxide nanocomposites, Chem. Eng. J. 350 (2018) 120–130.
[141] A.A.B. Christus, A. Ravikumar, P. Panneerselvam, K. Radhakrishnan, A novel Hg (II) sensor based on Fe3O4@ZnO nanocomposite as peroxidase mimics, Appl. Surf. Sci. 449 (2018) 669–676.
[142] A.A.B. Christus, P. Panneerselvam, A. Ravikumar, N. Morad, S. Sivanesan, Colorimetric determination of Hg(II) sensor based on magnetic nanocomposite (Fe3O4@ZIF-67) acting as peroxidase mimics, J. Photochem. Photobiol., A 364 (2018) 715–724.
[143] S. Zhang, H. Li, Z. Wang, J. Liu, H. Zhang, B. Wang, Z. Yang, A strongly coupled Au/Fe3O4/GO hybrid material with enhanced nanozyme activity for highly sensitive colorimetric detection, and rapid and efficient removal of Hg2+ in aqueous solutions, Nanoscale 7 (2015) 8495–8502.
[144] H. Yang, Y. Xiong, P. Zhang, L. Su, F. Ye, Colorimetric detection of mercury ions using MnO2 nanorods as enzyme mimics, Anal. Methods 7 (2015) 4596–4601.
[145] Y. Lu, J. Yu, W. Ye, X. Yao, P. Zhou, H. Zhang, S. Zhao, L. Jia, Spectrophotometric determination of mercury(II) ions based on their stimulation effect on the peroxidase-like activity of molybdenum disulfide nanosheets, Microchim. Acta 183 (2016) 2481–2489.
[146] G.-L. Wang, X.-F. Xu, L.-H. Cao, C.-H. He, Z.-J. Li, C. Zhang, Mercury(ii)-stimulated oxidase mimetic activity of silver nanoparticles as a sensitive and selective mercury(ii) sensor, RSC Adv. 4 (2014) 5867–5872.
[147] D.-F. Chai, Z. Ma, Y. Qiu, Y.-G. Lv, H. Liu, C.-Y. Song, G.-G. Gao, Oxidase-like mimic of Ag@Ag3PO4 microcubes as a smart probe for ultrasensitive and selective Hg2+ detection, Dalton Trans. 45 (2016) 3048–3054.